Journal of Inflammation Research

Dovepress
Taylor & Francis Group

Open Access Full Text Article

ORIGINAL RESEARCH

Exploring The Role of TOP2A in the Intersection of Pathogenic Mechanisms Between Rheumatoid Arthritis and Idiopathic Pulmonary Fibrosis Based on Bioinformatics

Shoujie Shi[1,2,*], Xin Hong[1,2,*], Yue Zhang[1,2,*], Shuilin Chen[1,2], Xiangfei Huang[3], Guihao Zheng[1,2], Bei Hu[1,2], Meifeng Lu[1,2], Weihua Li[1,2], Yanlong Zhong[1,2], Guicai Sun[1,2], Yulong Ouyang[1,2]

[1]Department of Sports Medicine, Orthopaedic Hospital, The First Affiliated Hospital, Jiangxi Medical College, Nanchang University, Nanchang, Jiangxi Province, People's Republic of China; [2]Artificial Joints Engineering and Technology Research Center of Jiangxi Province, Nanchang, Jiangxi Province, 330006, People's Republic of China; [3]Anesthesiology Department, The First Affiliated Hospital, Jiangxi Medical College, Nanchang University, Nanchang, Jiangxi Province, People's Republic of China

*These authors contributed equally to this work

Correspondence: Yulong Ouyang; Guicai Sun, Email ndyfy10126@ncu.edu.cn; ndsfy0740@ncu.edu.cn

Background: Rheumatoid arthritis (RA) and idiopathic pulmonary fibrosis (IPF) share a common pathogenic mechanism, but the underlying mechanisms remain ambiguous. Our study aims at exploring the genetic-level pathogenic mechanism of these two diseases.

Methods: We carried out bioinformatics analysis on the GSE55235 and GSE213001 datasets. Machine learning was employed to identify candidate genes, which were further verified using the GSE92592 and GSE89408 datasets, as well as quantitative real-time PCR (qRT-PCR). The expression levels of TOP2A in RA and IPF in vitro models were confirmed using Western blotting and qRT-PCR. Furthermore, we explored the influence of TOP2A on the occurrence and development of RA and IPF by using the selective inhibitor PluriSIn #2 in an in vitro model. Finally, an in vivo model of RA and IPF was constructed to assess TOP2A expression levels via immunohistochemistry.

Results: Our bioinformatics analysis suggests a potential intersection in the pathogenic mechanisms of RA and IPF. We have identified 7 candidate genes: CXCL13, TOP2A, MMP13, MMP1, LY9, TENM4, and SEMA3E. Our findings reveal that the expression level of TOP2A is significantly elevated in both in vivo and in vitro models of RA and IPF. Additionally, our research indicates that PluriSIn #2 can effectively restrain inflammatory factors, extracellular matrix deposition, migration, invasion, the expression and nuclear uptake of p-smad2/3 protein in RA and IPF in vitro models.

Conclusion: There is a certain correlation between RA and IPF at the genetic level, and the molecular mechanisms of their pathogenesis overlap, which might be the reason for the progression of RA. Among the candidate genes we identified, TOP2A may influence the occurrence and development of RA and IPF through the TGF-β/Smad signal pathway. This could be beneficial to the study of the pathogenesis and treatment of RA and IPF.

Keywords: rheumatoid arthritis, idiopathic pulmonary fibrosis, machine learning, TOP2A, fibrosis

Introduction

Rheumatoid arthritis (RA), a prevalent systemic autoimmune disorder, belongs to the category of connective tissue diseases (CTD).[1,2] It affects the normal functioning of bones and joints, resulting in a decline in the quality of life for patients.[2] Although all CTDs may cause the occurrence of interstitial lung disease (ILD), patients with RA have a greater risk of developing ILD.[3] Epidemiological studies have indicated that 60–80% of patients with RA also endure RA-associated interstitial lung disease (RA-ILD), and lung disease constitutes 10–20% of all-cause mortality.[4] Genetic,[5] humoral[6] and

Received: 24 September 2024
Accepted: 4 March 2025
Published: 11 March 2025

Graphical Abstract

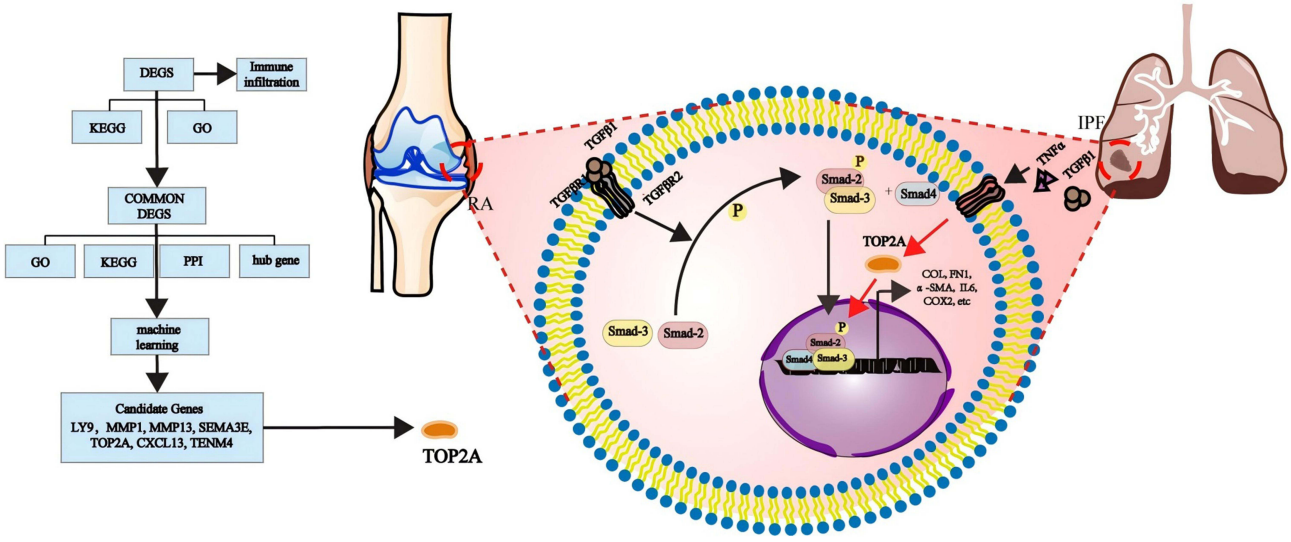

environmental factors[7] are regarded as being associated with RA-ILD, yet their etiological and pathological mechanisms have not been fully comprehended.

Not only can RA cause ILD, but other immune diseases, drugs, and chemical particles can also lead to the occurrence and development of ILD. Of course, there is also an ILD of unknown origin, which is known as idiopathic interstitial pneumonia (IIP).[8] IPF is an IIP patient presenting pulmonary pathological changes in UIP, and its prognosis is extremely poor.[9] IPF is an interstitial lung disease featuring high mortality, and its morbidity and mortality increase sharply with advancing age.[10,11] At present, it is generally acknowledged that the pathogenesis of IPF involves the injury of alveolar epithelial cells, followed by the secretion of fibrosis factors, which induces the differentiation and activation of myofibroblasts, thereby leading to the deposition and structural disorder of extracellular matrix (ECM).[12] Unfortunately, the molecular mechanism of IPF remains unclear, which results in the absence of an effective treatment for IPF at present.

RA-ILD and IPF are different diseases, but they share several clinical, imaging and genetic features.[13] Many studies further substantiate the possible connection between the two diseases.[14,15] Among all the histopathological patterns of RA-ILD, usual interstitial pneumonia (UIP) is the most prevalent pattern.[16] And UIP is also an ILD pattern necessary for a diagnosis of IPF.[9] This might imply that some molecular mechanisms of the progression from RA to RA-ILD may overlap with those of the development of IPF. Currently, an increasing number of studies have started to focus on the relationship between RA and IPF. Olivia's Mendelian randomized study identified a causal relationship between RA and IPF.[17] In light of the aforementioned research, the aim of this study is to identify the shared molecular markers of the two diseases through machine learning, in vivo and in vitro investigations, and to explore the common molecular mechanism underlying the occurrence and development of the two diseases.

Methods

Dataset Download and Preprocessing

We used the terms "rheumatoid arthritis" and "idiopathic pulmonary fibrosis" to search for gene expression profiles in the Gene Expression Omnibus (GEO) (http://www.ncbi.nlm.nih.gov/geo/) database respectively. The RA dataset GSE55235 and the IPF dataset GSE213001 both originate from the GEO database. The total mRNA of GSE55235 was extracted from synovial tissue and that of GSE213001 was extracted from lung tissue. These tissues are all from humans. We transformed the two datasets by log2 and annotated the genes for subsequent expression profile analysis.[18]

Identification of Shared Genes and Protein-Protein Interaction Network Generation

We identified the differentially expressed genes (DEGs) in RA and IPF through the "limma" package (|log FC|>1, adjusted P value<0.05).[19] We used "Venn Diagram" package to screen the differential genes up-regulated and down-regulated in both IPF and RA.[20] Visualization of protein-protein interactions was performed by the STRING database (version 11.5, with a minimum required interaction score of 0.4). Functional enrichment of the common differentially expressed genes (DEGs) and hub genes in IPF and RA was analyzed by Gene Ontology (GO) and Kyoto Encyclopedia of Genes and Genomes (KEGG) analysis. The hub gene was screened by the cytoHubba algorithm, and module analysis was conducted by the MCODE algorithm in Cytoscape software (version 3.9.1). The hub gene was used to predict interaction genes and build a network in the GeneMANIA database (https://genemania.org/).

Machine Learning

We utilized least absolute shrinkage and selection operator (LASSO) regression and support vector machine (SVM) learning to identify potential candidate genes associated with the diagnosis of IPF and RA. These two machine learning approaches establish decision boundaries through distinct calculation methods.[21–23] The intersection of the two results can serve as a candidate gene for diagnosis. The prognostic value of the candidate genes was further assessed by dataset GSE92592 and GSE89408 as well as ROC analysis. An AUC value > 0.7 was regarded as a good diagnostic effect.

Immunocytes Infiltration Analysis

We employed the CIBERSORT tool to assess the infiltration of 22 immunocytes based on gene expression profiles.[24] The proportion and difference of immunocytes infiltration between the disease group and the control group were analyzed. We established the correlation between candidate genes and immunocytes through Spearman analysis.

Cell Culture and Treatment

Human A549 non-small cell lung cancer cells and human SW982 synovial sarcoma cells were purchased from Procell (Wuhan, Hubei Province, China). The cells were cultured at 37°C in a 5% CO2-humidified incubator and were grown in high glucose Dulbecco's Modified Eagle Medium (DMEM) containing 10% FBS and 100 U/mL penicillin-streptomycin (Solarbio, Beijing, China). A549 cells were treated with 10 ng/mL human recombinant TGF-β1 protein (HY-P7118, Med Chem Express, Shanghai, China) in high glucose DMEM containing 10% FBS for 48 hours to induce the model of IPF. SW982 cells were treated with 2 ng/mL human recombinant TNF-α protein (HY-P7118, Med Chem Express, Shanghai, China) in high glucose DMEM containing 10% FBS for 48 hours to induce the model of RA.[25] Cells were treated with or without 20μM PluriSIn #2 (Med Chem Express, Shanghai, China) treatment.

Real-Time Polymerase Chain Reaction (Real-Time PCR) Assay

Total RNA was extracted from cells using RNAiso plus reagent (Takara, Japan) according to the manufacturer's instructions. RNA (1 μg) was reverse-transcribed to complementary DNA using All-in-One First-Strand cDNA Synthesis SuperMix (Trans Gen Biotech, Beijing, China). Green qPCR Super Mix Trans Gen Biotech, Beijing, China) and CFX Connect Real-Time PCR Detection System (Bio-Rad, California, United States) was used for real-time PCR. The primers used for amplification are listed in the table below (Table 1).

Western Blotting

The proteins were separated on 10% SDS-PAGE gel. Subsequently, the isolated protein was transferred to the PVDF membrane (Pall, NewYork, United States). The proteins transferred to the membrane were sealed with sealing fluid at room temperature for 2 hours, washed with TBS-T, and incubated with primary antibodies for 4 hours overnight. After washing with TBS-T, they were incubated with horseradish peroxidase labeled goat anti-rabbit or anti-mouse IgG (Proteintech, Wuhan, China) at room temperature for 2 h. Protein bands were displayed by enhanced chemiluminescence (UE Landy, Shanghai, China). The antibodies used in this process are as follows: Display of protein bands by enhanced chemiluminescence (Bio-Rad, California, United States). COL I (Proteintech, 66761-1-Ig, Wuhan, China, 1:800), COL III (Abcam, ab184993, Cambridge, Britain, 1:1000), FN1 (Proteintech, 66042-1-Ig, Wuhan, China, 1:5000), β-ACTIN

Table 1 The Sequences of Primer Pairs Used in the Study

Gene	Forward	Reverse
H-*gapdh*	GGAAGCTTGTCATCAATGGAAATC	TGATGACCCTTTTGGCTCCC
H-*col1a1*	CCCCTGGAAAGAATGGAGATG	AGCTGTTCCGGGCAATCCT
H-*col3a1*	CCCCGTATTATGGAGATGAACC	CCATCAGGACTAATGAGGCTTTC
H-*vimentin*	GGAGGAGATGCTTCAGAGAGAG	GGATTTCCTCTTCGTGGAGTTTC
H-*fn1*	GGAGAGTGGAAGTGTGAGAGGC	TCCATTTGAGTTGCCACCGT
H-*il6*	ATGAGGAGACTTGCCTGGTGAA	CTCTGGCTTGTTCCTCACTACTCTC
H-*cox2*	CGG TGAAACTCTGGCTAGACAG	GCAAACCGT AGATGCTCAGGGA
H-*top2a*	CCTTCTATGGTGGATGGTTTGA	ATGGGCTGCAAGAGGTTTAGAT
H-*tenm4*	GCCATCGTCATCTCAGCCACT	CCTCCGTGATCTCATACATCTGC
H-*ly9*	CCTACAAAGCCCAGATAAACCAA	CGTGGACGGACAACTTTTCAAT
H-*sema3e*	GCACATTATCACCTTGCTCCTG	TTTTAGAGCTGTACTCGGCCA

(Proteintech, 66009-1-Ig, Wuhan, China, 1:50000), VIMENTIN (Proteintech, 10366-1-AP, Wuhan, China, 1:5000), p-SMAD2/3 (Cell Signaling Technology, #8828, Boston, United States, 1:1000), SMAD2/3 (Cell Signaling Technology, #8685, Boston, United States, 1:1000), COX-2 (Proteintech, 66351-1-Ig, Wuhan, China, 1:5000), IL-6 (Afftiny, DF6087-BP, Cincinnati, United States).

High Density Cultivation and Alixin Blue Staining

We resuspended 3 × 10^6 cells in 500 μL of the culture medium and dropped 10 μL into each 24-well plate. After 1 hour of cultivation, the cells adhered to the wall and 800 μL of the complete culture medium was gently added. The cells were stimulated with TGF-β1 or PluriSIn #2 for 5 days, and then stained with Alizarin blue.

Migration and Invasion Assays

Used a 24-hole plate with a transwell membrane filter insert (JET, Guangdong, China) that either does not contain or contains pre-coated diluted base glue (servicebio, Wuhan, China). 1×10^4 cells/holes were inoculated in a serum-free medium and into the upper chamber of the 24-hole transwell chamber. SW982 cells were treated with TNF-α or PluriSIn #2 for 48 hours, then fixed with 10% formalin for 30 minutes and stained with 0.1% crystal violet for 30 minutes.

Immunocytochemistry

SW982 and A549 were cultured on confocal plates. When the confluence reached 20%, the cells were stimulated with or without TNF-α or TGF-β at 37 °C for 12 hours. Then, the cells were fixed in 4% paraformaldehyde for 30 minutes and washed with PBS three times. The cells were treated in 0.2% TritonX-100 solution for 15 minutes and washed with PBS three times. The cells were incubated with 5% bovine serum albumin (BSA, Solarbio, Beijing, China) for 1 hour at 37 °C. The antibody was diluted at a ratio of 1:200 and incubated with the antibody overnight at 4 °C. The next day, it was washed with PBS three times, incubated in the dark with 488-conjugated Goat anti-Rabbit IgG (Abclonal, AS053, Boston, United States, 1:200) for 2 hours, and then washed with PBS three times. The nucleus was stained with DAPI (Merck, Darmstadt, Germany) for 15 minutes and washed three times. Subsequently, the Anti-fluorescence quenching sealing tablet (servicebio, G1401, Wuhan, China) was used to prevent fluorescence quenching. The fluorescence expression of the cells was randomly obtained using a fluorescence confocal microscope (Leica, Wetzlar, Germany).

In Vivo Animal Experiment

The animal experiments were approved by the Animal Ethics Committee of the First Affiliated Hospital of Nanchang University (approval number: CDYFY-IACUC202404QR006). All experiments involving laboratory animals were conducted in accordance with the guidelines established by the Animal Experiment Ethics Committee of the First Affiliated Hospital of Nanchang University and the Guide for the Care and Use of Laboratory Animals.

We established an in vivo model of RAs in C57BL/6J mouse. Complete Freund's adjuvant (containing 5 mg/mL inactivated binding mycobacteria) and 2 mg/mL chicken type II collagen were emulsified and 0.1 mL was subcutaneously injected in the tail of each C57BL/6J mouse for three weeks and the injection was repeated. In the seventh week, the successful mice were selected by observing the degree of ankle swelling, and the ankle joints of the control group and the RA group (5 per group) were obtained.

We established an in vivo model of pulmonary fibrosis in C57BL/6J mouse. After anesthetizing the C57 mice, we used a video laryngoscope to assist the nebulizer to enter the oral cavity and sprayed bleomycin hydrochloride (5mg/kg) into the lungs of the mice through the nebulizer from below the glottis.

Immunohistochemical

The bone tissue was soaked in EDTA decalcification solution for 1 month, and the decalcification solution was changed every 3–7 days. The wax blocks were cut into 5 μm sections for immunohistochemical (IHC). The slices were dewaxed with xylene and hydrated with ethanol. The sections were boiled with 0.01% sodium citrate buffer to repair the antigen. After incubation with hydrogen peroxide, the cells were sealed with 5%BSA at room temperature for 1 hour. The antibody diluted by 5%BSA was incubated overnight at 4°C. The slides were treated with sheep anti-mouse/rabbit IgG (Jinqiao Biotechnology, Beijing, China). Then the cells were stained with DAB and re-stained with hematoxylin. The slides are sealed in neutral resin with cover slides for subsequent detection. The image of the tissue section was captured by imaging system (Shunyu instrument company, Zhejiang, China).

Statistical Analysis

Data were analyzed with the R 4.3.0 (https://www.rproject.org/), Cytoscape software (version 3.9.1), Perl 5.32.1 (https://www.perl.org) and R Bioconductor packages. Data were analyzed either by *t*-test or ANOVA. All statistical P values were two-sided, with $P < 0.05$ considered statistically significant.

Results

Identification of DEGs in RA and IPF

We employed a heat map to display the up-regulated and down-regulated genes within the top 50 of the two diseases (Figure 1A and B). In GSE213001, there were 971 downregulated and 1208 upregulated genes in the IPF group (Figure 1C and D). Compared to the control group, there were 2179 DEGs in the IPF group and 1056 DEGs in RA. In GSE 55235, there were 465 downregulated and 591 upregulated genes in the RA group. Finally, 67 co-up-regulated genes and 38 co-down-regulated genes were identified in the two diseases (Figure 1E).

GO Analysis and KEGG Analysis

We conducted GO and KEGG analyses of the common DEGs to explore their potential biological information (Figure 2A and B). KEGG was enriched in 32 pathways, including the IL-17 signaling pathway, cytokine-cytokine receptor interaction, relaxin signaling pathway, and so forth. GO was enriched in 629 biological processes (BP), 21 cellular components (CC), and 65 molecular functions (MF), including collagen metabolic process, fibrillar collagen trimer, extracellular matrix structural constituent conferring tensile strength, and so on.

Identification of Hub Gene

We utilized the common DEGs to construct a highly reliable PPI network (PPI enrichment p-value < 1.0E-16, Figure 2C). We identified the first 15 hUB genes through the "cytoHubba" algorithm (Figure 2D). 15 hub genes and 20 interacting genes were evaluated by GeneMANIA to predict interaction molecules and functions (Figure 2E). We discovered that many proteins related to the extracellular matrix are closely associated with the pathogenesis of the two diseases. Finally, our circular diagram demonstrates the enrichment of the functions and pathways of the hub gene, including collagen metabolism, extracellular matrix organization, IL-17 signaling, and so on (Figure 2G and F).

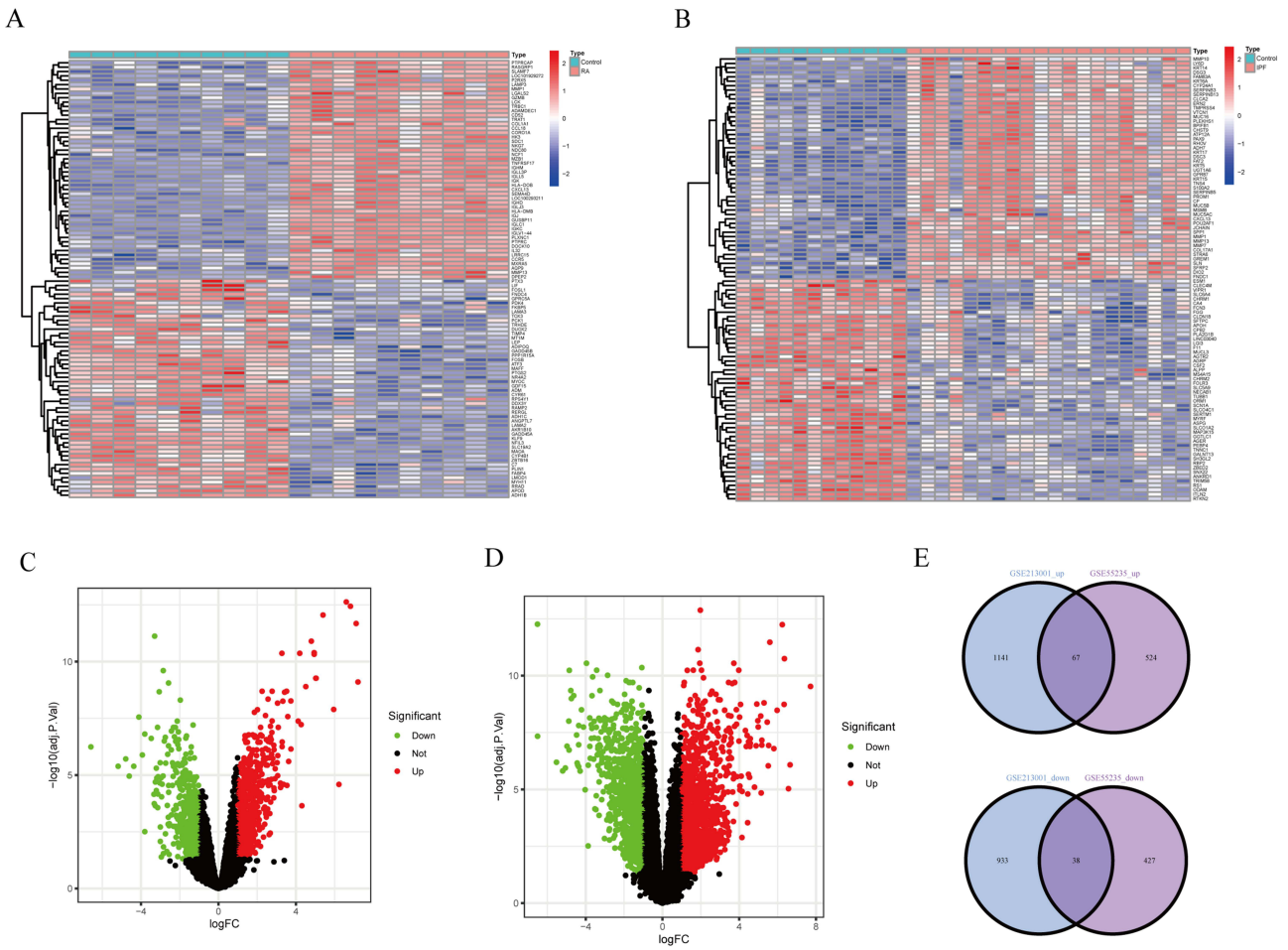

Figure 1 Identification of DEGs in RA and IPF. (**A**) Heatmap of the expression levels of the gene between RA and the control. (**B**) Heatmap of the expression levels of the gene between IPF and the control. (**C**) Volcanic plot of the expression levels of the gene between RA and the control. (**D**) Volcanic plot of the expression levels of the gene differences between IPF and the control. (**E**) co-up-regulated and co-down-regulated genes in the two diseases.

Identification of Candidate Genes

Eleven candidate genes were identified through Lasso regression analysis, and 13 candidate genes were identified by the SVM algorithm. Seven identical candidate genes were screened out by the two types of machine learning, including C-X-C Motif Chemokine Ligand 13 (CXCL13), DNA topoisomerase IIA (TOP2A), Matrix Metallopeptidase 13 (MMP13), MMP1, Lymphocyte Antigen 9 (LY9), Teneurin Transmembrane Protein 4 (TENM4), and Semaphorin 3E (SEMA3E) (Figure 3A and C). Subsequently, we employed GSE92592 and GSE89408 to verify the candidate genes. We verified whether the expression level of these genes in the new sequencing results was consistent with the dataset we analyzed and verified the diagnostic effect of these genes through the ROC curve (Figure 3D–G).

Immunocytes Infiltration Analysis

Immunocytes are involved in the pathogenesis of RA and IPF, so we analyzed the effects of immunocytes on the pathogenesis of the two diseases. The proportion of immunocytes infiltration between RA and IPF and the control group is shown in Figures 4A and C. Compared with the control group, the levels of mast cells activated, neutrophils, NK cells activated, plasma cells, T cells CD4 memory activated, T cells CD4 memory resting, T cells CD8 and T cells follicular helper in the RA group were significantly different from those in the control group (Figure 4B). He levels of B cells naïve, dendritic cells activated, macrophages M2, monocytes, NK cells resting, and plasma cells were significantly different in the IPF group (Figure 4D). Then, we established the relationship between candidate genes and immunocytes, and observed the effects of different candidate genes on immunocytes (Figures 1s and 2s). The expression of TOP2A

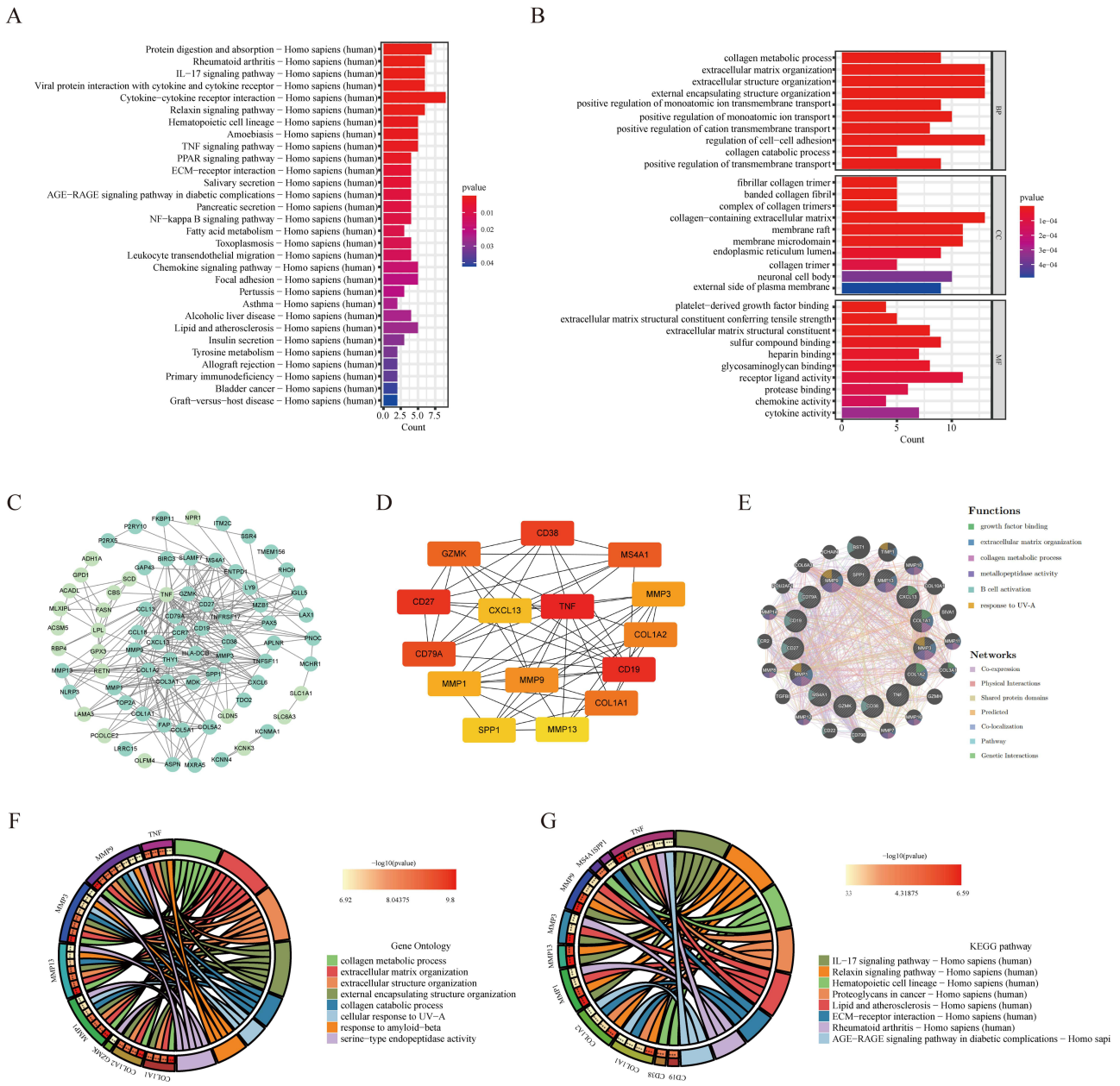

Figure 2 GO and KEGG analysis of DEGs and hub genes. (**A**) KEGG analysis of the DEGs. (**B**) GO analysis of the DEGs. (**C**) The PPI network of up-regulated and down-regulated shared genes (Dark green is the up-regulated gene and light green is the down-regulated gene). (**D**) The PPI network of 15 hub genes. (**E**) GeneMANIA predict the relationships between co-expression, shared protein domain, co-location, and pathway. (**F**) GO analysis of the hub genes. (**G**) KEGG analysis of the hub genes.

gene was closely related to M2 macrophages, plasma cells, Monocytes, and Dendritic cells activated in RA (Figure 4E). The results showed that the expression of TOP2A gene was closely related to Plasma cells, T cells CD8, T cells follicular helper, Neutrophils, T cells CD4 naïve, T cells regulatory (Tregs), T cells CD4 memory resting, and Mast cells activated in IPF (Figure 4F).

Expression Level of Candidate Genes in RA and IPF Models in Vitro

We utilized TNF-α to establish the in vitro model of RA and TGF-β to establish the in vitro model of IPF. qRT-PCR demonstrated that the expression levels of *ly9, sema3e*, and t*op2a* were significantly different in the IPF and RA groups. The expression level of Tenm4 was only increased in the RA in vitro model (Figure 5A and B). TOP2A not only conforms to the prediction results, but its role in these two diseases has also been reported.[26,27] However, the mechanism of action has not

https://doi.org/10.2147/JIR.S497734

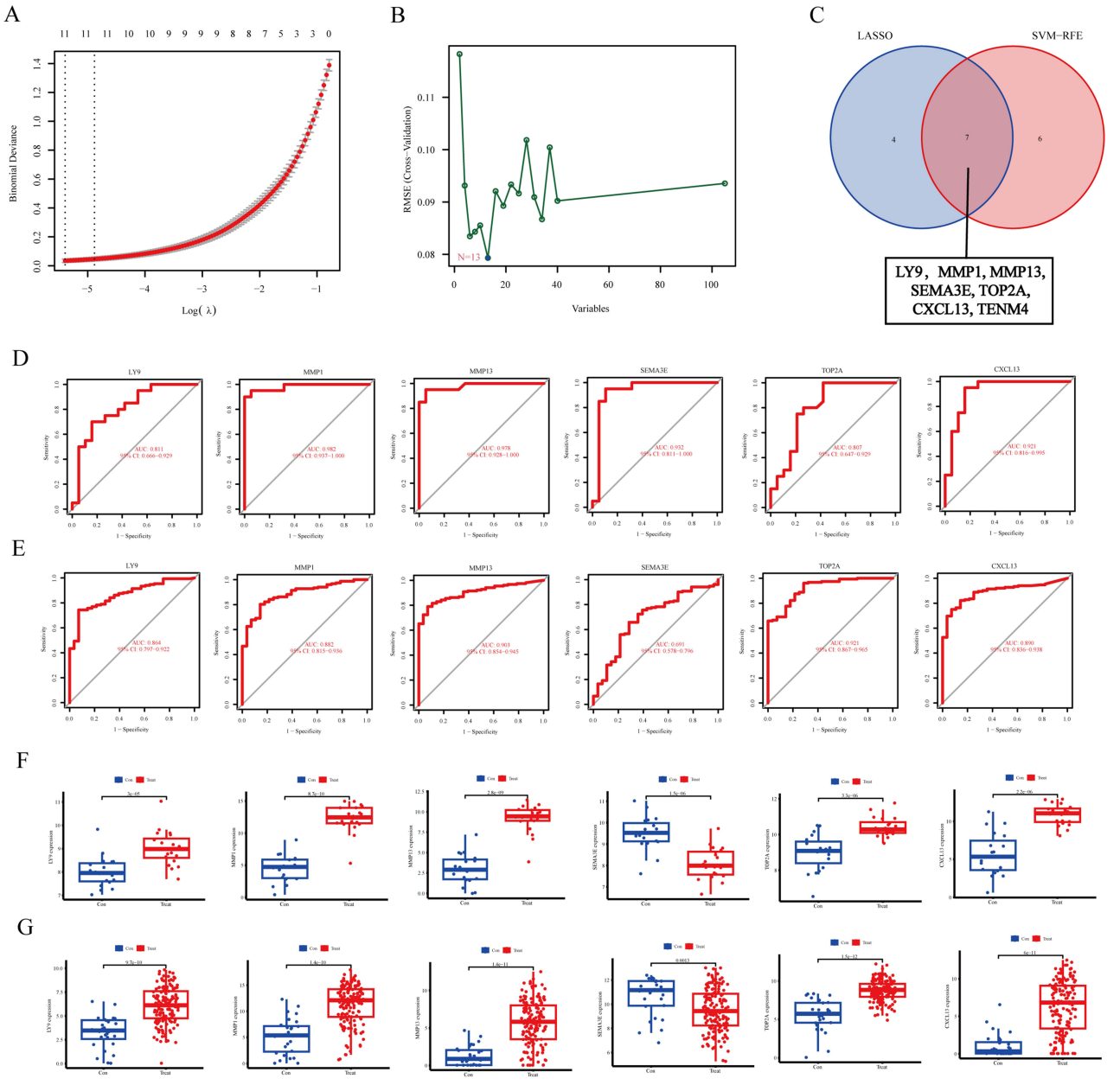

Figure 3 Identification of candidate genes. (**A**) Screening of key genes through Lasso regression analysis. (**B**) Screening of key genes by SVM learning. (**C**) Candidate genes identified in the LASSO model and SVM learning. (**D**) The ROC curve of candidate genes for GSE92592. (**E**) The ROC curve of candidate genes for GSE89408. (**F**) The expression level of candidate genes in GSE92592. (**G**) The expression level of candidate genes in GSE89408.

been clearly elucidated. Hence, we have developed a strong interest in the role of TOP2A in the two diseases. We employed Western blotting to detect fibrosis and inflammation-related indicators to validate the establishment of the in vitro model. Simultaneously, we detected the protein expression level of TOP2A, and the results revealed that the expression level of top2a was also significantly elevated in the in vitro models of the two diseases (Figure 5C and D).

TOP2A Inhibitor Alleviate Fibrosis Induced by TGF-β in A549

As a selective inhibitor of TOP2A, PluriSin #2 does not directly inhibit the activity of TOP2A but selectively inhibits its transcription, thereby significantly reducing the level of the TOP2A protein.[28] We then verified the effect of PluriSIn #2 on the IPF model in vitro. The increased secretion of the extracellular matrix is the main pathological process in the progression of pulmonary fibrosis. The results of qRT-PCR and Western Blotting demonstrated that TGF-β could induce fibrosis in A549, while

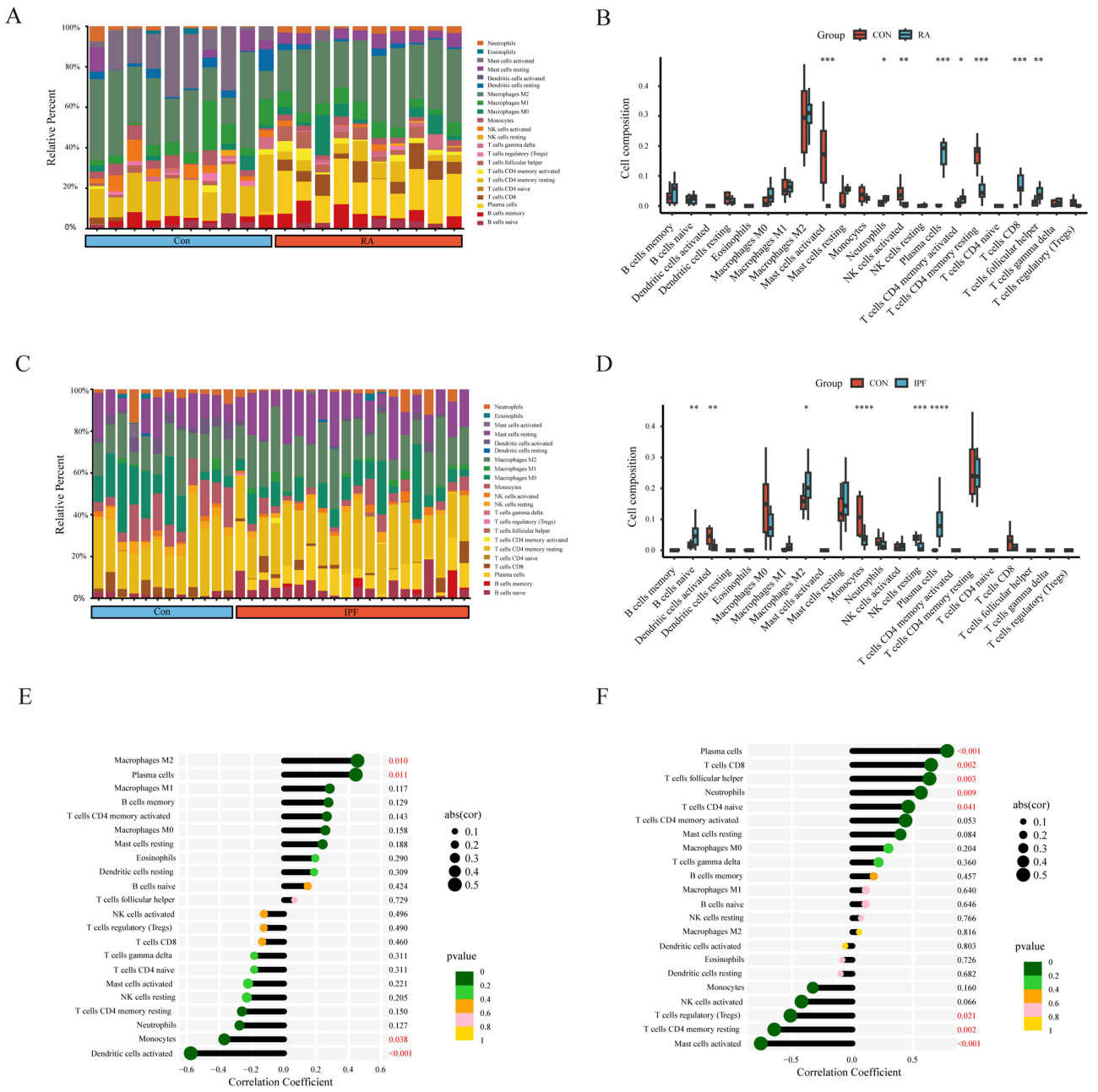

Figure 4 Immunocytes infiltration analysis. (**A**) The bar plot shown the proportion of 22 immunocytes in RA. (**B**) Levels of infiltrating immunocytes in RA and control groups (*P<0.05, **P<0.01, ***P<0.001). (**C**) The bar plot shown the proportion of 22 immunocytes in IPF. (**D**) Levels of infiltrating immunocytes in IPF and control groups (*P<0.05, **P<0.01, ***P<0.001, ****P<0.0001). (**E**) The lollipop plot shown the relationship between TOP2A genes and immunocytes in IPF. (**F**) The lollipop plot shown the relationship between TOP2A genes and immunocytes in RA.

PluriSIn #2 could inhibit the mRNA and protein expression levels of VIMENTIN, COL I, COL III, and FN1 (Figure 6A and B). Not only that, we also discovered that PluriSIn #2 could alleviate the deposition of the extracellular matrix through high-density culture and Alcian blue staining (Figure 6C).

TOP2A Inhibitors Alleviate the Inflammatory Response, Fibrosis, Migration and Invasion of SW982 Induced by TNF- α

We employed PluriSIn #2 to inhibit the expression of TOP2A while SW982 was stimulated by TNF-α, and to observe the effect of TOP2A inhibition on the in vitro model of RA. Our qRT-PCR results indicated that PluriSIn#2 could

https://doi.org/10.2147/JIR.S497734

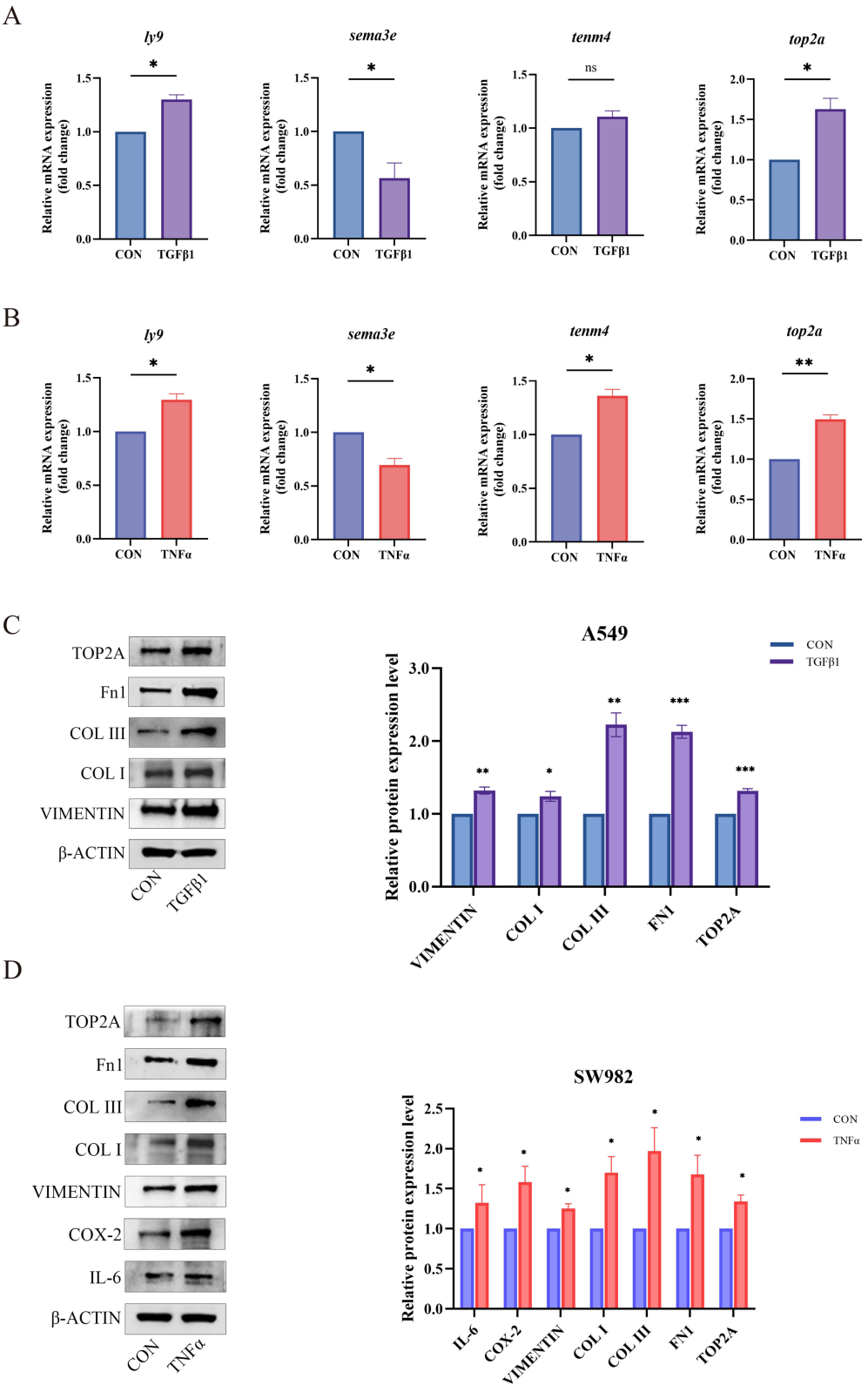

Figure 5 Expression level of candidate genes in RA and IPF models in vitro. (**A**) qRT-PCR detected *ly9, sema3e, tenm4*, and *top2a* mRNA expression level of IPF model in vitro (*P<0.05, **P<0.01). (**B**) qRT-PCR detected *ly9, sema3e, tenm4*, and *top2a* mRNA expression level of RA model in vitro. (**C**) Western blotting results of VIMENTIN, COL I, COL III, FN1, TOP2A protein expression level in IPF vitro model. (**D**) Western blotting results of IL-6, COX-2, VIMENTIN, COL I, COL III, FN1, TOP2A protein expression level in RA vitro model (*P<0.05, **P<0.01, ***P<0.001).

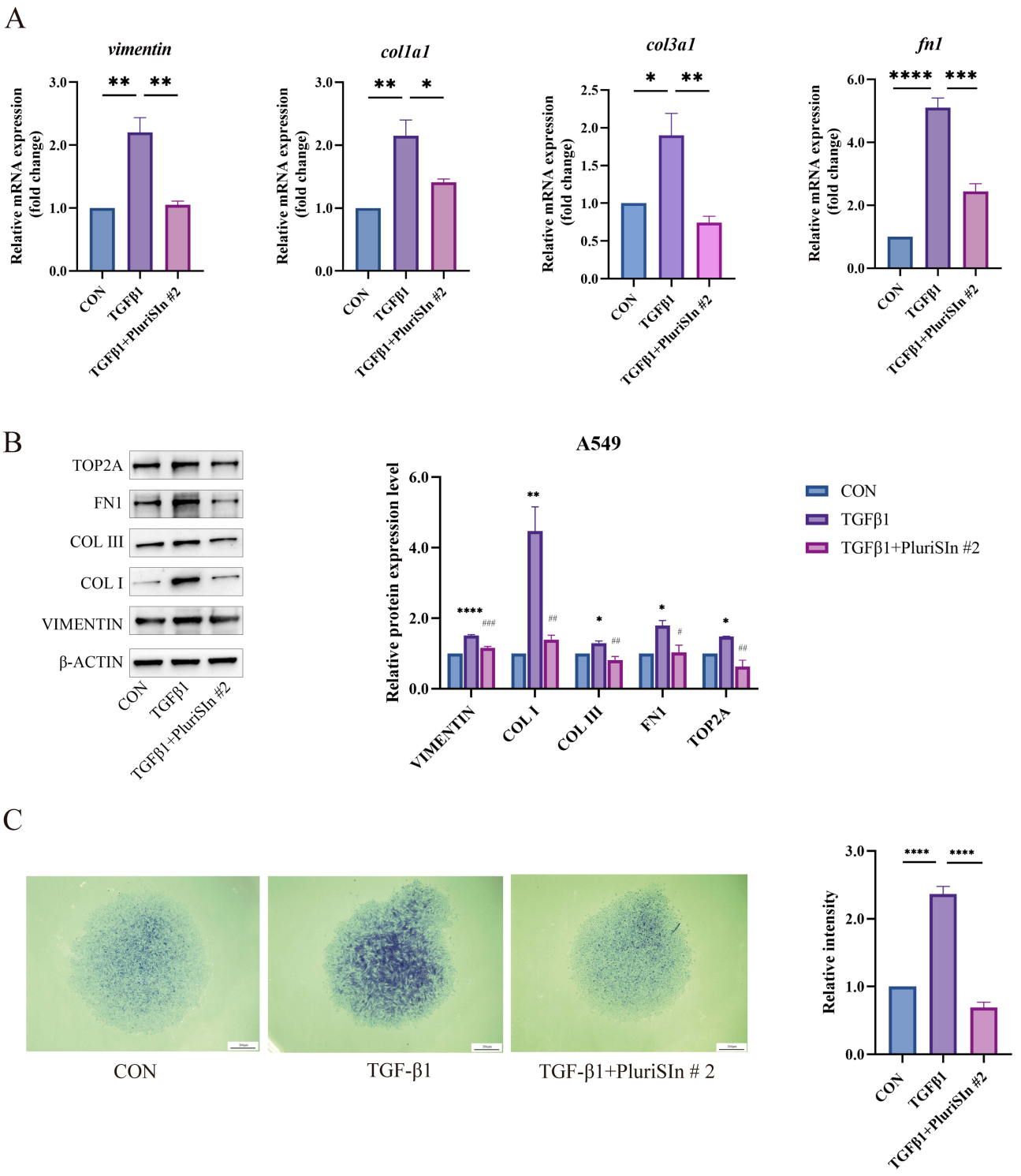

Figure 6 TOP2A inhibitors alleviate fibrosis induced by TGF-β in A549. (**A**) qRT-PCR detected the mRNA expression levels of *vimentin, col1a1*, *col3a1*, and *fn1* in the IPF in vitro model with PluriSin #2 (*<0.05, **<0.01, ***<0.001, ****<0.0001). (**B**) Western blotting results of the protein expression levels of VIMENTIN, COL I, COL III, and FN1 in the RA in vitro model with PluriSin #2 (*:TGF-β1 vs Con, #: vs TGF-β1+PluriSin #2 vs TGF-β1, *<0.05, **<0.01, ***<0.001, ****<0.0001, #<0.05, ##<0.01, ###<0.001). (**C**) High-density culture and alcian blue staining show the effect of extracellular matrix deposition in A549 with PluriSin #2 (****<0.0001).

https://doi.org/10.2147/JIR.S497734

significantly suppress the expression of *col1a1, col3a1, fn1, vimentin, il-6*, and *cox-2* mRNA in SW982 induced by TNF-α (Figure 7A). We also found that PluriSIn #2 could also inhibit the protein expression of COL I, COL III, VIMENTIN, FN1, IL-6 and COX-2 in RA in vitro by Western-Blotting (Figure 7B). These results suggest that TOP2A inhibitor can alleviate the fibrosis and inflammatory progression during the occurrence and development of RA. Moreover, the invasion and migration of synovium play an important role in the occurrence and development of RA (Figure 7C). Our results show that PluriSIn#2 can also inhibit the migration and invasion of SW982 stimulated by TNF-α. The above results indicate that TOP2A may be involved in the progress of RA.

TOP2A May Influence the Occurrence and Development of RA and IPF Through the TGF-β/Smad Signal Axis

The TGF-β/Smad signal pathway holds considerable significance in the pathogenesis of IPF and RA. We utilized immunofluorescence to detect the effect of PluriSIn #2 on p-smad2/3 entry and found that PluriSIn#2 was capable of inhibiting TNF-α-induced p-smad2/3 entry in SW982 cells and TGF-β-induced A549 cells (Figure 8A and C). At the same time, we determined the expression level of p-smad2/3 by Western blotting to investigate the effect of TOP2A on the TGF-β/Smad signal pathway. PluriSIn#2 could significantly repress the expression level of the TGF-β/Smad signal pathway (Figure 8B and D). Hence, we hypothesize that TOP2A might regulate the occurrence and development of RA and IPF by up-regulating the TGF-β/Smad signal pathway.

The Expression of TOP2A Increased During IPF Development in Vivo

Pathological examination was conducted on lung tissue sections of the IPF in vitro model. HE and Sirius Red staining showed that the lung tissue of IPF model mice was severely fibrotic, and the expression levels of COL I and COL III, which are related to fibrosis, were significantly increased. Moreover, the expression level of TOP2A in IPF mice was also significantly elevated (Figure 9A–C).

The Expression of TOP2A Increased During RA Development in Vivo

We developed a RA mouse model to explore the expression level of TOP2A in RA mice. HE and Sirius red staining showed that synovial hyperplasia in RA mice was more severe than that in sham-operated mice (Figure 10A and B). COLI and COL III are important indicators of synovial fibroblast activation and fibrosis, while IL-6 and COX2 are important indicators of RA. Subsequently, we performed immunohistochemical staining on the joints of mice. The results showed that compared with sham operation, the expression levels of COLI, COLIII, Fn1 and VIMENTIN, IL-6 and COX-2 in synovium of RA mice were significantly increased, which proved the effectiveness of RA model. At the same time, we found that the expression level of TOP2A in synovium of RA mice increased (Figure 10A and C).

Discussion

The pathogenesis of RA and IPF is unknown, which leads to poor treatment of the two diseases. Moreover, the complications of RA, RA-UIP and IPF, cause serious damage to public health. Therefore, it is of great significance to study the pathogenesis of IPF and RA from the genetic level. In recent years, many studies have attempted to clarify the pathogenesis of diseases by analyzing the comorbidity mechanism of two diseases through bioinformatics.[29,30] We first discussed the core genes and related pathways of IPF and RA-UIP. Then the candidate gene CXCL13, TOP2A, MMP13, MMP1, LY9, TENM4, SEMA3E was screened by machine learning.

CXCL13 is a secretory growth factor that functions in inflammation and can serve as a chemokine for neutrophils. An increase in serum CXCL13 levels seemingly indicates the occurrence of RA and the advancement of inflammation.[31] Not only that, CXCL13 may also affect the progress of IPF.[32] MMP13 and MMP1 are not only significant components in regulating the balance of the extracellular matrix but also crucial indicators of the progression of inflammation and fibrosis-related diseases. In both of these two diseases, both MMP1 and MMP13 demonstrated abnormal expression.[33–35]

LY9 (also known as CD229 or SLAMF3) belongs to the family of signal lymphoid activating molecules (SLAM) and plays an important role in the regulation of immune response.[36] LY9 is predominantly expressed in immunocytes and is

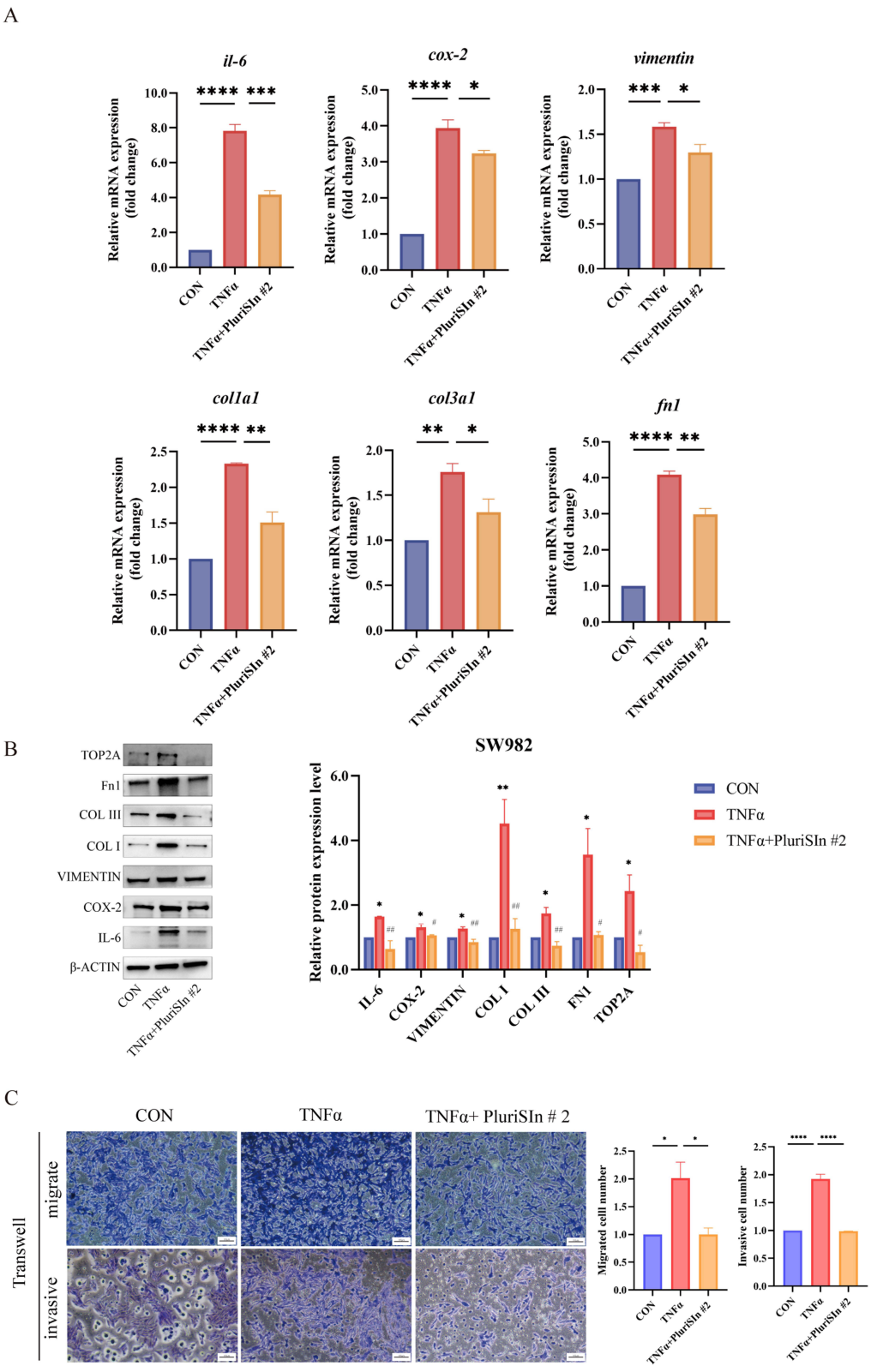

Figure 7 TOP2A inhibitors alleviate the inflammatory, fibrosis, migration and invasion of SW982 induced by TNF-α. (**A**) qRT-PCR detected the mRNA expression levels of *il-6, cox-2, vimentin, col1a1, col3a1*, and *fn1* in the RA in vitro model with PluriSin #2 (*P<0.05, **P<0.01, ***P<0.001, ****P<0.0001). (**B**) Western blotting results of the protein expression levels of IL-6, COX-2, VIMENTIN, COL I, COL III, and FN1 in the RA in vitro model with PluriSin #2(*: TNF-α vs Con, #: TNF-α+PluriSin #2 vs TNF-α, *P<0.05, **P<0.01, #P<0.05, ##P<0.01). (**C**) Comparison of migration and invasion through transwell in the RA in vitro model with PluriSin #2 (*P<0.05, ****P<0.0001).

https://doi.org/10.2147/JIR.S497734

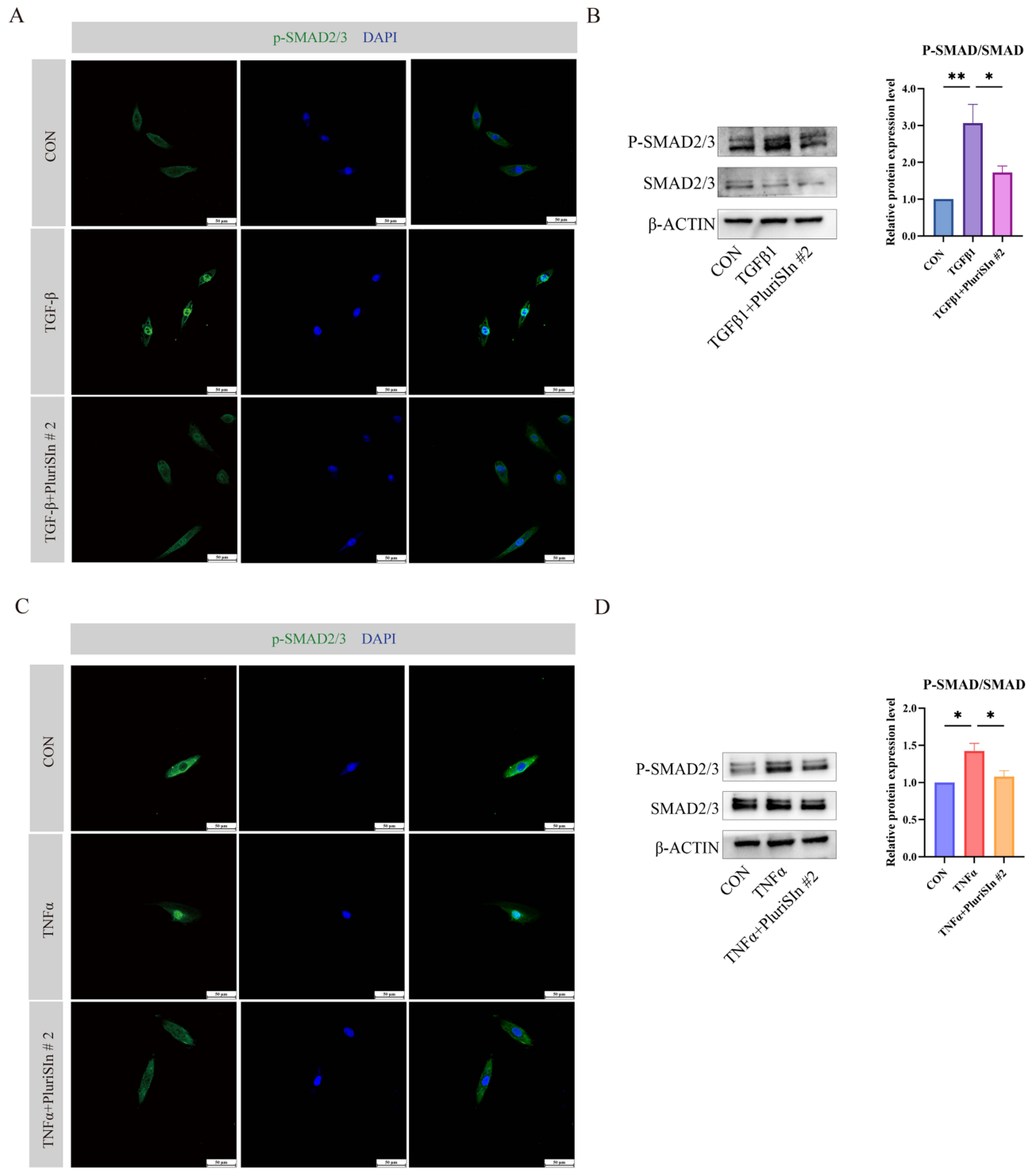

Figure 8 TOP2A inhibitors influence of RA and IPF in vitro through the TGF-β/Smad signal axis. (**A**) Immunofluorescence detects the effect of PluriSin #2 on the nuclear insertion of P-SMAD2/3 in vitro of IPF. (**B**) Western blotting results of the P-SMAD2/3 protein expression level in IPF. (**C**) Immunofluorescence detects the effect of PluriSin #2 on the nuclear insertion of P-SMAD2/3 in vitro of RA. (**D**) Western blotting results of the P-SMAD2/3 protein expression level in RA (*P<0.05, **P<0.01).

frequently implicated in the pathogenesis of autoimmune diseases and cancer.[37] Hu's study demonstrated that LY9 can be reversed by iguratimod through the JAK1/STAT3 pathway by promoting Th17 differentiation.[38] It has also been shown that LY9 promotes the invasive phenotype of multiple myeloma by activating the ERK signaling pathway.[39] However, most studies have shown that Ly9 mainly affects immunocytes and then affects the progression of the disease, rather than

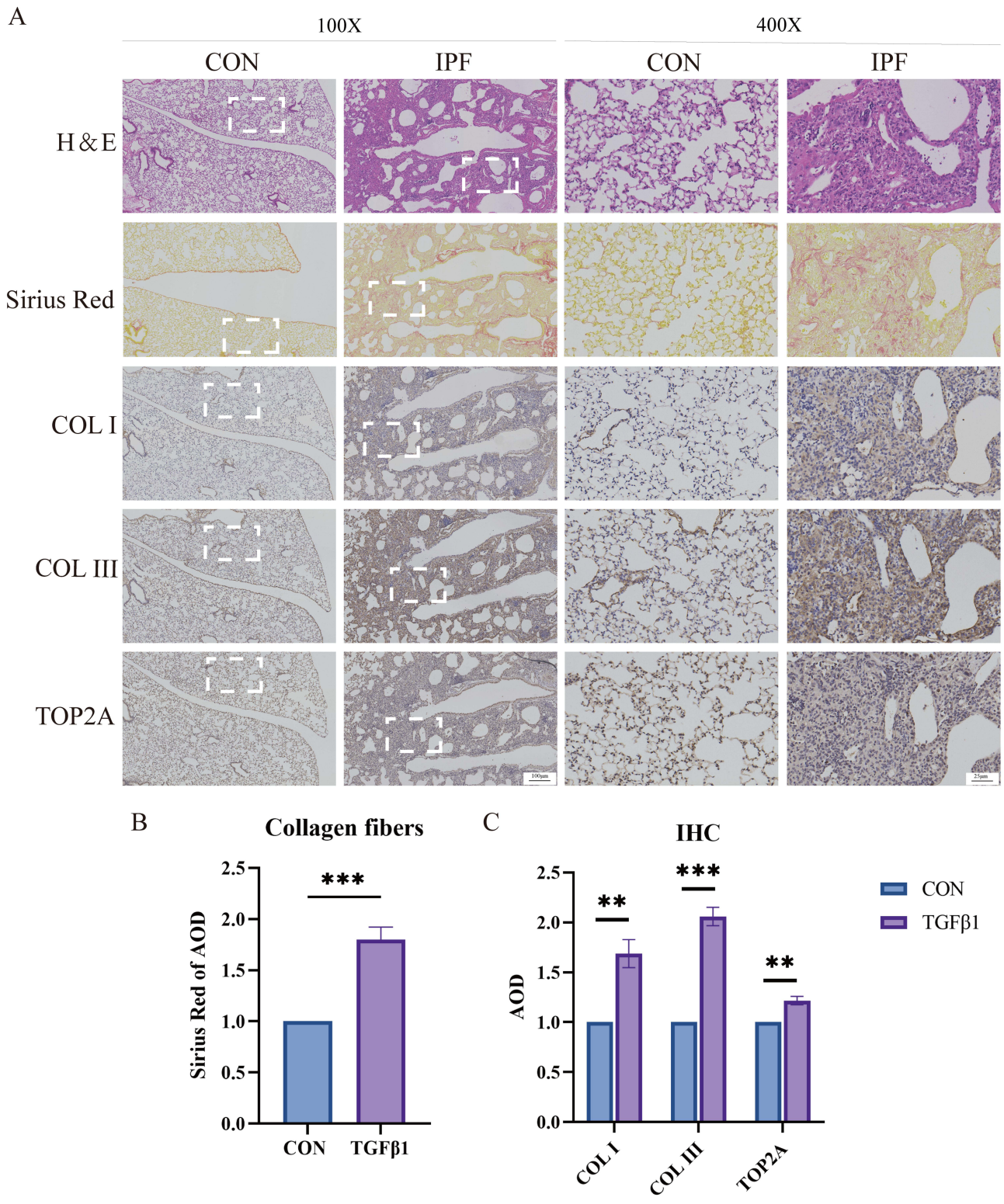

Figure 9 The expression of TOP2A increased during IPF development in vivo. (**A**) The expression levels of fibrosis, COL I, COL III, and TOP2A proteins were compared between the control group and the IPF group through HE staining, Sirius red staining, and immunohistochemistry. (**B**) Statistical chart of Sirius Red staining for the control group and the IPF group. (**C**) Statistical chart of immunohistochemistry for the control group and the IPF group (**<0.01, ***<0.001).

https://doi.org/10.2147/JIR.S497734

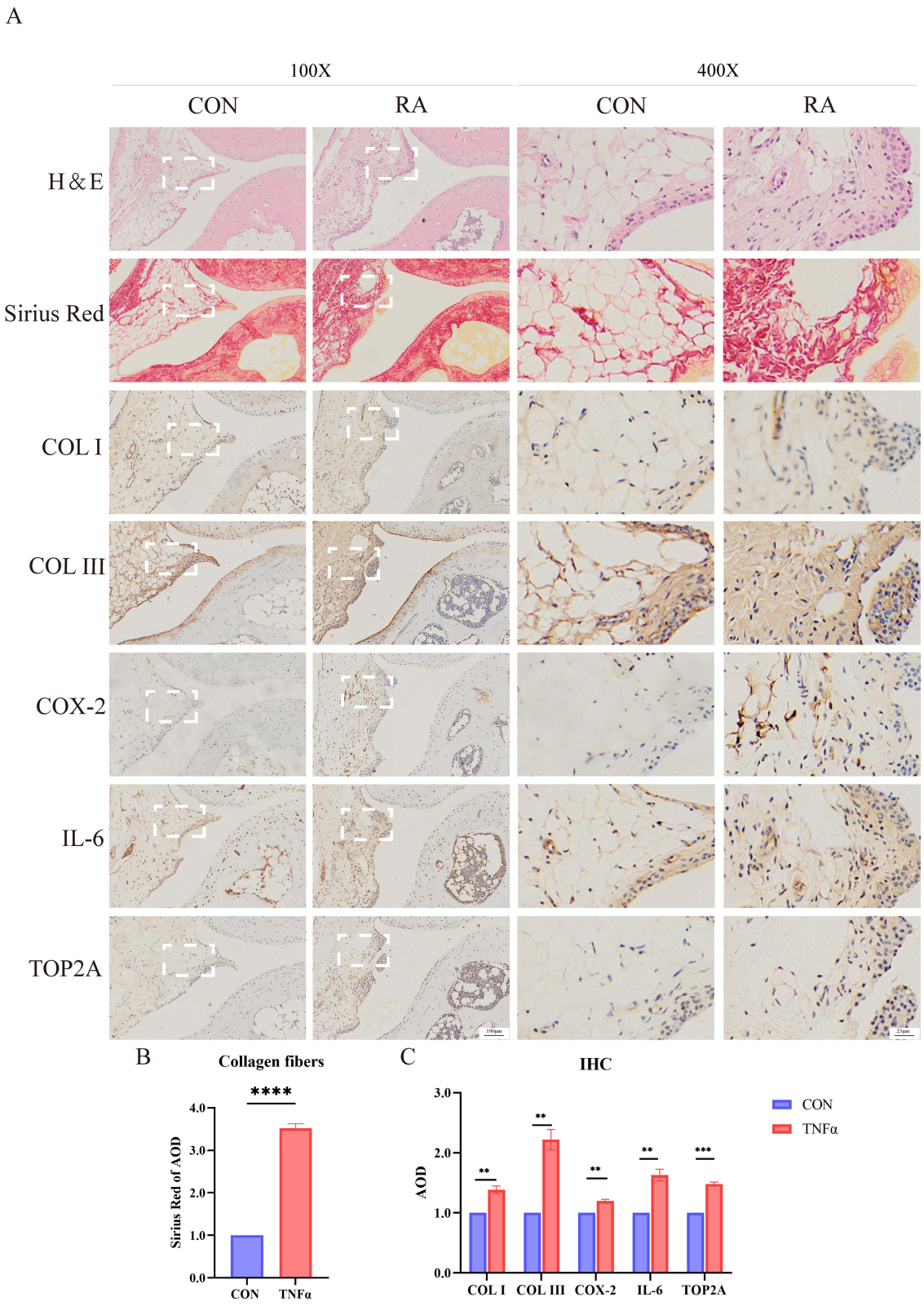

Figure 10 The expression of TOP2A increased during RA development in vivo. (**A**) The expression levels of fibrosis, COL I, COL III, IL6, and COX-2 proteins were compared between the control group and the RA group through HE staining, Sirius red staining, and immunohistochemistry. (**B**) Statistical chart of Sirius Red staining for the control group and the RA group. (**C**) Statistical chart of immunohistochemistry for the control group and the RA group (**<0.01, ***<0.001, ****<0.0001).

directly affecting the progression of the disease. The sequencing data analyzed in this study come from tissue transcriptome sequencing rather than single cell sequencing, so the difference in LY9 expression may be caused by immunocytes.

TENM4 is a type II transmembrane protein that is highly expressed in the central nervous system and is involved in nerve development and connection establishment.[40] TENM4 regulates integrin β 1-FAK signal transduction and affects the formation of myelin sheath in small diameter axons.[40] TENM4 might be co-expressed with the TGF-β1 gene, thereby accelerating the reconstruction of engineered tendon tissue at the histological level.[41] This characteristic might imply that it is implicated in the pathogenesis of RA and IPF.

SEMA3 are secretory proteins that regulate synaptic and dendritic development.[42] Moreover, SEMA4A, SEMA4D and SEMA3 are potential biomarkers and therapeutic candidates for RA, and they may be targets for inflammation and angiogenesis in RA.[43] SEMA3 pathway may also affect the occurrence and development of RA by regulating immune.[44] The specific molecular mechanism of SEMA3 in RA disease has not been elaborated in detail, and there are few studies on IPF. An in-depth study of SEMA3 will be conducive to clarifying the pathogenesis of RA and IPF.

In addition to the above genes, we found an interesting gene TOP2A. TOP2A is an enzyme that control and alter the topological states of DNA during transcription.[45] TOP2A is aberrantly expressed in numerous cancer diseases, such as lung cancer, nasopharyngeal carcinoma, ovarian cancer, and so forth.[46–48] Moreover, numerous studies have investigated the specific mechanism of the influence of TOP2A on the occurrence and development of diseases. Wang's study discovered that TOP2A promotes the migration, invasion, and epithelial-mesenchymal transformation of cervical cancer cells by activating the PI3K/AKT signal transduction.[49] TOP2A can also influence the growth, proliferation, migration and invasion of colorectal cancer, glioma and pancreatic cancer via the Wnt/β-catenin signal pathway.[50–52] TOP2A also can accelerate the progression of high-grade serous ovarian cancer by regulating TGF- β/SMAD pathway.[53] The Wnt pathway and the TGF-β pathway are significant pathways influencing the extracellular matrix, and the imbalance of the extracellular matrix is also the primary mechanism of fibrosis. These molecular mechanisms are also crucial processes in RA and IPF.[54,55] Therefore, we conjecture that TOP2A might influence the progression of IPF and RA. We detected the elevated expression of TOP2A in both diseases through bioinformatics analysis, in vivo and in vitro experiments, and verified that TOP2A affected the inflammatory and fibrotic phenotypes of RA and IPF cell lines. We also discovered that selective transcriptional inhibitors of TOP2A can impact the activation of the TGF-β/Smad signaling pathway in vitro. TOP2A might become a crucial biomarker of the pathogenesis of RA and IPF, and influence the progression of the two diseases via the TGF-β/Smad signal pathway. Future studies will deeply investigate the specific molecular mechanism of the impacts of TOP2A on the two diseases, which will assist in clarifying the etiology of RA and IPF, and offer an effective target for the targeted therapy of the two diseases.

Although our research has attempted to explain the pathogenesis of IPF and RA from the genetic level and selected the candidate gene TOP2A to verify the mechanism, our research still has the following limitations. Firstly, we detected the expression levels of TOP2A, LY9, TENM4, and SEMA3E by qRT-PCR, but some of the results were not consistent with the bioinformatics results. This might be attributed to the fact that the in vitro models of IPF and RA are not completely in line with the real pathogenesis. The test results of the in vitro model of TOP2A that we chose for in-depth study are consistent with the sequencing results. Secondly, we examined the effect of TOP2A on the entry and expression of p-smad2/3 in vitro and proved that TOP2A could regulate the TGF-β/Smad signal pathway, but this has not been confirmed by rescue experiments that TOP2A affected the progression of the disease by regulating the TGF-β/Smad signal pathway. The in-depth study of its mechanism is of great significance to the future research on the pathogenesis and treatment of RA and IPF. Finally, verifying the correlation between the expression levels of TOP2A at different disease stages and disease progression at the organizational level may enable TOP2A to become a potential biomarker for the diagnosis of the two diseases. However, our research is still far from sufficient to transform TOP2A into a potential diagnostic marker and therapeutic approach for the two diseases. This might imply the abnormal expression of TOP2A in organ fibrosis. In the future, it is hoped that the team researching pulmonary fibrosis will pay attention to the TOP2A gene, which may offer a novel idea for the study of IPF.

Conclusion

There is a certain correlation between RA and IPF at the genetic level, and the molecular mechanisms of their pathogenesis overlap, which might be the reason for the progression of RA. Among the candidate genes we identified, TOP2A may influence the occurrence and development of RA and IPF through the TGF-β/Smad signal pathway. This could be beneficial to the study of the pathogenesis and treatment of RA and IPF.

Data Sharing Statement

All relevant data and materials are freely available to any investigator on request.

Ethics Declarations

The animal experiments were approved by the Animal Ethics Committee of the First Affiliated Hospital of Nanchang University (approval number: CDYFY-IACUC202404QR006).

According to the requirements of Article 32 of the "Measures for Ethical Review of Life Science and Medical Research Involving Human Subjects" issued by the National Health Commission, the Ministry of Education, the Ministry of Science and Technology, and the National Administration of Traditional Chinese Medicine (2023), research involving human life science and medical research that uses legally obtained publicly available data or data generated through observation without interfering with public behavior can be exempted from ethical review. The use of the database in our research was reviewed and approved by the Ethics Committee of the First Affiliated Hospital of Nanchang University, and the ethics application was waived.

Acknowledgments

The GSE55235, GSE213001, GSE92592 and GSE89408 datasets were obtained from the GEO database.

Funding

This work is supported by the National Natural Science Foundation of China (No. 82260870).

Disclosure

The authors declare no conflicts of interest in this work.

References

1. Baig M, Wong LK, Zia AW, Wu H. Development of biomedical hydrogels for rheumatoid arthritis treatment. *Asian J Pharm Sci*. 2024;19:100887. doi:10.1016/j.ajps.2024.100887
2. Sparks JA. Rheumatoid Arthritis. *Ann Intern Med*. 2019;170:Itc1–itc16.
3. Fischer A, du Bois R. Interstitial lung disease in connective tissue disorders. *Lancet*. 2012;380:689–698. doi:10.1016/S0140-6736(12)61079-4
4. Kanat F, Levendoglu F. Teke T: radiological and functional assessment of pulmonary involvement in the rheumatoid arthritis patients. *Rheumatol Int*. 2007;27:459–466. doi:10.1007/s00296-006-0234-0
5. Nogee LM, Dunbar AE, Wert SE, Askin F, Hamvas A, Whitsett JA. A mutation in the surfactant protein C gene associated with familial interstitial lung disease. *N Engl J Med*. 2001;344:573–579. doi:10.1056/NEJM200102223440805
6. Mori S, Koga Y, Sugimoto M. Different risk factors between interstitial lung disease and airway disease in rheumatoid arthritis. *Respir Med*. 2012;106:1591–1599. doi:10.1016/j.rmed.2012.07.006
7. Saag KG, Kolluri S, Koehnke RK, et al. Rheumatoid arthritis lung disease. Determinants of radiographic and physiologic abnormalities. *Arthritis Rheum*. 1996;39:1711–1719. doi:10.1002/art.1780391014
8. Dubey S, Woodhead F. Survival differences in rheumatoid arthritis interstitial lung disease and idiopathic pulmonary fibrosis may be explained by delays in presentation: results from multivariate analysis in a monocentric UK study. *Rheumatol Int*. 2024;44:99–105. doi:10.1007/s00296-023-05505-0
9. American Thoracic Society. Idiopathic pulmonary fibrosis: diagnosis and treatment. International consensus statement. American Thoracic Society (ATS), and the European Respiratory Society (ERS). *Am J Respir Crit Care Med*. 2000;161:646–664. doi:10.1164/ajrccm.161.2.ats3-00
10. Martinez FJ, Collard HR, Pardo A, et al. Idiopathic pulmonary fibrosis. *Nat Rev Dis Primers*. 2017;3:17074. doi:10.1038/nrdp.2017.74
11. Mei Q, Liu Z, Zuo H, Yang Z, Qu J. Idiopathic pulmonary fibrosis: an update on pathogenesis. *Front Pharmacol*. 2021;12:797292. doi:10.3389/fphar.2021.797292
12. Phan SH. Biology of fibroblasts and myofibroblasts. *Proc Am Thorac Soc*. 2008;5:334–337. doi:10.1513/pats.200708-146DR
13. Matson S, Lee J, Eickelberg O. Two sides of the same coin? A review of the similarities and differences between idiopathic pulmonary fibrosis and rheumatoid arthritis-associated interstitial lung disease. *Eur Respir J*. 2021;57.

14. Seibold MA, Wise AL, Speer MC, et al. A common MUC5B promoter polymorphism and pulmonary fibrosis. *N Engl J Med*. 2011;364:1503–1512. doi:10.1056/NEJMoa1013660
15. Juge PA, Borie R, Kannengiesser C, et al. Shared genetic predisposition in rheumatoid arthritis-interstitial lung disease and familial pulmonary fibrosis. *Eur Respir J*. 2017;49.
16. Cavagna L, Monti S, Grosso V, et al. The multifaceted aspects of interstitial lung disease in rheumatoid arthritis. *Biomed Res Int*. 2013;2013:759760. doi:10.1155/2013/759760
17. Leavy OC, Kawano-Dourado L, Stewart ID, et al. Rheumatoid arthritis and idiopathic pulmonary fibrosis: a bidirectional Mendelian randomisation study. *Thorax*. 2024;79:538–544. doi:10.1136/thorax-2023-220856
18. Gautier L, Cope L, Bolstad BM. Irizarry RA: affy--analysis of Affymetrix GeneChip data at the probe level. *Bioinformatics*. 2004;20:307–315. doi:10.1093/bioinformatics/btg405
19. Smyth GK. Limma: linear Models for Microarray Data. In: Gentleman R, Carey VJ, Huber W, Irizarry RA, Dudoit S, editors. *Bioinformatics and Computational Biology Solutions Using R and Bioconductor*. New York: Springer New York; 2005:397–420.
20. Jia A, Xu L, Wang Y. Venn diagrams in bioinformatics. *Brief Bioinform*. 2021;22.
21. Yang C, Delcher C, Shenkman E, Ranka S. Machine learning approaches for predicting high cost high need patient expenditures in health care. *Biomed Eng Online*. 2018;17:131. doi:10.1186/s12938-018-0568-3
22. Aruna S, R SP. A novel SVM based CSSFFS feature selection algorithm for detecting breast cancer. *Int J Comput Appl*. 2011;31(8):14–20.
23. Noble WS. What is a support vector machine? *Nat Biotechnol*. 2006;24:1565–1567. doi:10.1038/nbt1206-1565
24. Newman AM, Liu CL, Green MR, et al. Robust enumeration of cell subsets from tissue expression profiles. *Nat Methods*. 2015;12:453–457. doi:10.1038/nmeth.3337
25. Khansai M, Phitak T, Klangjorhor J, et al. Effects of sesamin on primary human synovial fibroblasts and SW982 cell line induced by tumor necrosis factor-alpha as a synovitis-like model. *BMC Complement Altern Med*. 2017;17:532. doi:10.1186/s12906-017-2035-2
26. Fang Q, Li T, Chen P, et al. Comparative analysis on abnormal methylome of differentially expressed genes and disease pathways in the immune cells of RA and SLE. *Front Immunol*. 2021;12:668007. doi:10.3389/fimmu.2021.668007
27. García-Martín A, Navarrete C, Garrido-Rodríguez M, et al. EHP-101 alleviates angiotensin II-induced fibrosis and inflammation in mice. *Biomed Pharmacother*. 2021;142:112007. doi:10.1016/j.biopha.2021.112007
28. Ben-David U, Cowell IG, Austin CA, Benvenisty N. Brief reports: controlling the survival of human pluripotent stem cells by small molecule-based targeting of topoisomerase II alpha. *Stem Cells*. 2015;33:1013–1019. doi:10.1002/stem.1888
29. Liao Y, Peng X, Yang Y, et al. Exploring ABHD5 as a lipid-related biomarker in idiopathic pulmonary fibrosis: integrating Machine Learning, bioinformatics, and in vitro experiments. *Inflammation*. 2024. doi:10.1007/s10753-024-02107-1
30. Liao Y, Yang Y, Zhou G, et al. Anoikis and SPP1 in idiopathic pulmonary fibrosis: integrating bioinformatics, cell, and animal studies to explore prognostic biomarkers and PI3K/AKT signaling regulation. *Expert Rev Clin Immunol*. 2024;20:679–693. doi:10.1080/1744666X.2024.2315218
31. Bugatti S, Manzo A, Benaglio F, et al. Serum levels of CXCL13 are associated with ultrasonographic synovitis and predict power Doppler persistence in early rheumatoid arthritis treated with non-biological disease-modifying anti-rheumatic drugs. *Arthritis Res Ther*. 2012;14:R34.
32. Adegunsoye A, Alqalyoobi S, Linderholm A, et al. Circulating plasma biomarkers of survival in antifibrotic-treated patients with idiopathic pulmonary fibrosis. *Chest*. 2020;158:1526–1534. doi:10.1016/j.chest.2020.04.066
33. Craig VJ, Zhang L, Hagood JS, Owen CA. Matrix metalloproteinases as therapeutic targets for idiopathic pulmonary fibrosis. *Am J Respir Cell mol Biol*. 2015;53:585–600. doi:10.1165/rcmb.2015-0020TR
34. Frank S, Peters MA, Wehmeyer C, et al. Regulation of matrixmetalloproteinase-3 and matrixmetalloproteinase-13 by SUMO-2/3 through the transcription factor NF-κB. *Ann Rheum Dis*. 2013;72:1874–1881. doi:10.1136/annrheumdis-2012-202080
35. Checa M, Ruiz V, Montaño M, Velázquez-Cruz R, Selman M, Pardo A. MMP-1 polymorphisms and the risk of idiopathic pulmonary fibrosis. *Hum Genet*. 2008;124:465–472. doi:10.1007/s00439-008-0571-z
36. Calpe S, Wang N, Romero X, et al. The SLAM and SAP gene families control innate and adaptive immune responses. *Adv Immunol*. 2008;97:177–250. doi:10.1016/S0065-2776(08)00004-7
37. Zhou T, Guan Y, Sun L, Liu W. A review: mechanisms and molecular pathways of signaling lymphocytic activation molecule family 3 (SLAMF3) in immune modulation and therapeutic prospects. *Int Immunopharmacol*. 2024;133:112088. doi:10.1016/j.intimp.2024.112088
38. Hu P, Cai J, Yang C, et al. SLAMF3 promotes Th17 differentiation and is reversed by iguratimod through JAK1/STAT3 pathway in primary Sjögren's syndrome. *Int Immunopharmacol*. 2024;126:111282. doi:10.1016/j.intimp.2023.111282
39. Ishibashi M, Takahashi R, Tsubota A, et al. SLAMF3-mediated signaling via ERK pathway activation promotes aggressive phenotypic behaviors in multiple myeloma. *mol Cancer Res*. 2020;18:632–643. doi:10.1158/1541-7786.MCR-19-0391
40. Suzuki N, Fukushi M, Kosaki K, et al. Teneurin-4 is a novel regulator of oligodendrocyte differentiation and myelination of small-diameter axons in the CNS. *J Neurosci*. 2012;32:11586–11599. doi:10.1523/JNEUROSCI.2045-11.2012
41. Tu T, Shi Y, Zhou B, et al. Type I collagen and fibromodulin enhance the tenogenic phenotype of hASCs and their potential for tendon regeneration. *NPJ Regen Med*. 2023;8:67.
42. Matrone C, Ferretti G. Semaphorin 3A influences neuronal processes that are altered in patients with autism spectrum disorder: potential diagnostic and therapeutic implications. *Neurosci Biobehav Rev*. 2023;153:105338. doi:10.1016/j.neubiorev.2023.105338
43. Avouac J, Pezet S, Vandebeuque E, et al. Semaphorins: from angiogenesis to inflammation in rheumatoid arthritis. *Arthritis Rheumatol*. 2021;73:1579–1588. doi:10.1002/art.41701
44. Wang J, Liu C, Wang T, et al. Single-cell communication patterns and their intracellular information flow in synovial fibroblastic osteoarthritis and rheumatoid arthritis. *Immunol Lett*. 2023;263:1–13. doi:10.1016/j.imlet.2023.09.005
45. Wang JC. Cellular roles of DNA topoisomerases: a molecular perspective. *Nat Rev mol Cell Biol*. 2002;3:430–440. doi:10.1038/nrm831
46. Zhang B, Li J, Wang Y, et al. Deubiquitinase USP7 stabilizes KDM5B and promotes tumor progression and cisplatin resistance in nasopharyngeal carcinoma through the ZBTB16/TOP2A axis. *Cell Death Differ*. 2024;31:309–321. doi:10.1038/s41418-024-01257-x
47. Wu J, Zhang L, Li W, et al. The role of TOP2A in immunotherapy and vasculogenic mimicry in non-small cell lung cancer and its potential mechanism. *Sci Rep*. 2023;13:10906. doi:10.1038/s41598-023-38117-6
48. Zhang K, Zheng X, Sun Y, et al. TOP2A modulates signaling via the AKT/mTOR pathway to promote ovarian cancer cell proliferation. *Cancer Biol Ther*. 2024;25:2325126. doi:10.1080/15384047.2024.2325126

49. Wang B, Shen Y, Zou Y, et al. TOP2A promotes cell migration, invasion and epithelial-mesenchymal transition in cervical cancer via activating the PI3K/AKT signaling. *Cancer Manag Res*. 2020;12:3807–3814. doi:10.2147/CMAR.S240577
50. Pei YF, Yin XM, Liu XQ. TOP2A induces malignant character of pancreatic cancer through activating β-catenin signaling pathway. *Biochim Biophys Acta Mol Basis Dis*. 2018;1864:197–207. doi:10.1016/j.bbadis.2017.10.019
51. Chen X, Lv X, Gao L, et al. Chalcone derivative CX258 suppresses colorectal cancer via inhibiting the TOP2A/Wnt/β-Catenin signaling. *Cells*. 2023;13:12. doi:10.3390/cells13010012
52. Liu Y, Ma J, Song JS, et al. DNA topoisomerase II alpha promotes the metastatic characteristics of glioma cells by transcriptionally activating β-catenin. *Bioengineered*. 2022;13:2207–2216. doi:10.1080/21655979.2021.2023985
53. Gao Y, Zhao H, Ren M, et al. TOP2A promotes tumorigenesis of high-grade serous ovarian cancer by regulating the TGF-β/Smad pathway. *J Cancer*. 2020;11:4181–4192. doi:10.7150/jca.42736
54. Cai S, Ming B, Ye C, et al. Similar transition processes in synovial fibroblasts from rheumatoid arthritis and osteoarthritis: a single-cell study. *J Immunol Res*. 2019;2019:4080735. doi:10.1155/2019/4080735
55. Favaloro EJ, Curnow J, Pasalic L, et al. Laboratory assessment of factor VIII inhibitors: when is it required? A perspective informed by local practice. *J Clin Med*. 2024;14(1):13. doi:10.3390/jcm14010013